Ostwald, R. J., MacLennan, D. H., & Dorrington, K. J. (1974) *J. Biol. Chem. 249*, 5867–5871.
Ronjat, M., & Ikemoto, N. (1989) *Biophys. J. 55*, 13a.
Saito, A., Seiler, S., Chu, A., & Fleischer, S. (1984) *J. Cell Biol. 99*, 875–885.
Scott, B. T., Simmerman, H. K. B., Collins, J. H., Nadal-Ginard, B., & Jones, L. R. (1988) *J. Biol. Chem. 263*, 8958–8964.
Slupsky, J. R., Ohnishi, M., Carpenter, M. R., & Reithmeier, R. A. F. (1987) *Biochemistry 26*, 6539–6544.
Smith, J. S., Imagawa, T., Ma, J., Fill, M., Campbell, K. P., & Coronado, R. (1988) *J. Gen. Physiol. 92*, 1–26.
Volpe, P., Cutweniger, H. E., & Montecucco, C. (1987) *Arch. Biochem. Biophys. 253*, 138–145.
Williams, R. W., & Beeler, T. J. (1986) *J. Biol. Chem. 261*, 12408–12413.

Competitive Binding of ATP and the Fluorescent Substrate Analogue 2′,3′-*O*-(2,4,6-Trinitrophenylcyclohexadienylidine)adenosine 5′-Triphosphate to the Gastric H^+,K^+-ATPase: Evidence for Two Classes of Nucleotide Sites†

Larry D. Faller

Center for Ulcer Research and Education, Department of Medicine, University of California at Los Angeles School of Medicine and Veterans Administration Hospital Center, Los Angeles, California 90073

Received September 13, 1988; Revised Manuscript Received January 13, 1989

ABSTRACT: ATP and the fluorescent substrate analogue TNP-ATP bind competitively to the gastric H,K-ATPase. Substrate and product completely reverse the fluorescence enhancement caused by TNP-ATP binding to the enzyme. The fluorophore is displaced monophasically from apoenzyme. However, ATP displaces TNP-ATP from the Mg^{2+}-quenched state in two steps of equal amplitude. The midpoints of the titrations differ by more than 2 orders of magnitude. The estimated substrate constants are in reasonable agreement with published Michaelis constants. TNP-ATP is not a substrate for the H,K-ATPase. The fluorophore prevents phosphorylation by ATP and competitively inhibits the K^+-stimulated pNPPase and ATPase activities of the enzyme. K_i is approximately the same for both hydrolytic activities and consistent with the K_d of TNP-ATP measured directly. K_m for pNPP is 1.48 ± 0.15 mM. Two Michaelis constants are required to fit the ATPase data: K_{m1} = 0.10 ± 0.01 mM and K_{m2} = 0.26 ± 0.05 mM.

The gastric proton pump is classified as an E_1E_2-type ATPase. The distinguishing characteristic of this class of active transport enzyme is the formation of a covalent phosphoenzyme intermediate. Another common feature of the calcium (Inesi et al., 1967; Yamamato & Tonomura, 1967), sodium (Kanazawa et al., 1970), and proton (Wallmark et al., 1980) pumps is increased catalytic efficiency at higher ATP concentrations. Early attempts to explain the latter phenomenon postulated two nucleotide sites, usually on interacting protomers of a dimeric structure. More recently it has been shown that the E_1 and E_2 conformers, which were originally proposed to explain catalysis–transport coupling and the physical translocation of ions, can also explain the substrate dependence of the hydrolysis reaction if the affinity of the enzyme for ATP is different in the E_1 and E_2 conformations (Smith et al., 1980). A critical issue in deciding between two-site mechanisms and one-site, two-state models is the number of nucleotide sites.

One approach to this problem is the use of fluorescent substrate analogues to count the number of nucleotide sites. TNP-ATP[1] is a fluorescent analogue of ATP that has been used extensively to investigate both the sodium (Moczydlowski & Fortes, 1981a,b) and calcium (Dupont et al., 1982, 1985; Watanabe & Inesi, 1982; Dupont & Pougeois, 1983; Nakamoto & Inesi, 1984; Bishop et al., 1984, 1987; Berman, 1986) pumps. Sartor showed the feasibility of using TNP-ATP to probe nucleotide sites on the H,K-ATPase also and reported preliminary evidence for only one class of TNP-ATP site in the absence of divalent cations, but both biphasic TNP-ATP binding and displacement by nucleotides in the presence of Mg^{2+} (Sartor et al., 1982). A reinvestigation of TNP-ATP binding to the H,K-ATPase has shown that Mg^{2+} causes a slow change in the conformation of the substrate analogue–enzyme complex without affecting the fluorophore dissociation constant significantly, or the number of binding sites (Faller, 1989). The number of TNP-ATP sites (N) was counted and found to be twice the stoichiometry of phosphoenzyme formation (E–P), suggesting that there may be two classes of nucleotide sites. The competition experiments reported in this paper provide additional support for a two-site interpretation of the N/E–P ratio.

†This work was supported by National Science Foundation Grant DMB 83-09756 and U.S. Public Health Service Grants DK 36873 and section C2 of program project AM 17328 (George Sachs overall principal investigator).

[1] Abbreviations: H,K-ATPase, Mg^+-dependent, H^+-transporting, and K^+-stimulated ATPase (EC 3.6.1.3); Na,K-ATPase, Mg^{2+}-dependent and Na^+- and K^+-stimulated ATPase; Ca-ATPase, Ca^{2+}- and Mg^{2+}-dependent ATPase; SR, sarcoplasmic reticulum; TNP-AXP, 2′,3′-*O*-(2,4,6-trinitrophenylcyclohexadienylidine)ATP or -ADP; AMP-PNP, adenyl-5′-yl imidodiphosphate; pNPP, *p*-nitrophenyl phosphate; $H_2VO_4^-$, vanadate ion; FITC, fluorescein 5′-isothiocyanate; eosin Y, 2′,4′,5′,7′-tetrabromofluorescein; omeprazole, 5-methoxy-2-{[(4-methoxy-3,5-dimethyl-2-pyridinyl)methyl]sulfinyl}-1*H*-benzimidazole.

0006-2960/89/0428-6771$01.50/0

Experimental Procedures

Materials

H,K-ATPase. The enzyme was isolated from hog stomachs and purified by step-gradient centrifugation. This method of preparing H,K-ATPase and evidence for homogeneity of the resulting enzyme's binding and catalytic properties have been described in detail (Faller, 1989). The phosphorylation capacity of the enzyme is 1.5 ± 0.3 nmol mg^{-1} (Faller et al., 1983). The specific activity of the five H,K-ATPase preparations used in this study was 176 ± 47 μmol h^{-1} mg^{-1} of Lowry protein (Lowry et al., 1951).

Reagents. TNP-ATP and TNP-ADP were purchased from Molecular Probes. Their concentrations were determined spectrophotometrically at 408 nm by using an extinction coefficient of 2.64×10^4 M^{-1} cm^{-1}. [γ-^{32}P]ATP was obtained from ICN. Sodium orthovanadate from Fisher was used. Vanadate-free ATP, ADP, and pNPP were purchased from Sigma. All other reagents were of the highest grade available.

Methods

Fluorescence Measurements. Fluorescence measurements were made in a Perkin-Elmer MPF 44 spectrofluorometer with entrance and exit slit widths set at 10 nm. The instrument was equipped with a high-intensity cell holder and provision for continuous stirring at ambient temperature. TNP-ATP was excited at 405 nm, and the emitted light was detected after passage through a Corning CS 3-70 high-band-pass filter.

Kinetic Assays. The rate of pNPP hydrolysis was determined by quenching the reaction at desired time points with 0.1 N sodium hydroxide and measuring the amount of *p*-nitrophenolate ion produced spectrophotometrically. A colorimetric assay was also used to follow ATP hydrolysis at high concentrations of the substrate (Yoda & Hokin, 1970). To obtain the greater sensitivity required for assays at low ATP concentrations [γ-^{32}P]ATP was used, and the extracted $^{32}P_i$ was quantified by scintillation counting. The reaction time and enzyme concentration were adjusted so that no more than 20% hydrolysis occurred. Other details of the reaction mixtures are given in the figure legends.

A derivative-free, nonlinear least-squares program was used to fit

$$v_0 = V[S]_0/([S]_0 + K_m(app)) \quad (1)$$

for competitive inhibition, where

$$K_m(app) = K_m(1 + ([I]_0/K_i)) \quad (2)$$

to the experimental data. Square brackets are used to indicate molar concentration, and the subscript zero denotes total concentration. The other symbols are those recommended by the IUPAC/IUB Commission on Biochemical Nomenclature 1973). Analytically fitting the rate equation avoids the visual distortion that occurs when reciprocals are taken to linearize plots or rearrangements are made that introduce the dependent variable into both coordinates. It has the advantage of increasing the number of data points (n) used in the estimation of V, K_m, and K_i by fitting all substrate and inhibitor concentrations simultaneously.

Equations analogous to eq 2 describe the relationship between the apparent dissociation constant, measured when two ligands are competing for a site, and the true equilibrium dissociation constant (Segel, 1975). For example, if enzyme in the presence of a fixed concentration of substrate analogue is titrated with substrate, the subscript s replaces the subscript m in the expression relating the apparent [K_s(app)] and true (K_s) substrate constants. $[I]_0$ in eq 2 becomes the concentration of the fixed ligand (substrate analogue in the example), and the dissociation constant (K_d) of the substrate analogue is substituted for K_i.[2]

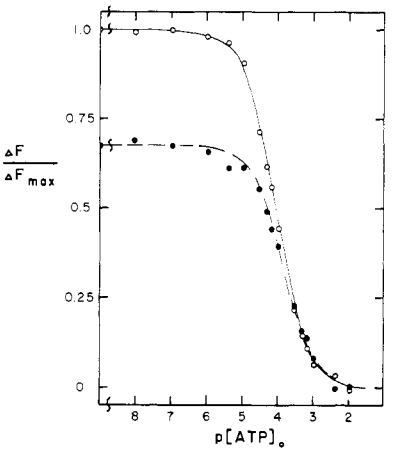

FIGURE 1: ATP displaces TNP-ATP. Enzyme loaded with fluorophore was titrated with ATP. $p[ATP]_0 = -\log [ATP]_0$. The ordinate is fraction of the enhancement observed when TNP-ATP binds in 0.8 mM EDTA. The theoretical curve through the open circles was calculated for ATP binding to a single class of sites on apoenzyme with K_s(app) = 86 μM. KCl (7 mM) was also present in the titration denoted by solid circles. This concentration of K^+ quenches the fluorescence 30–40%. K_s(app) = 145 μM gave the best fit to the titration curve in the presence of the monovalent cation. Other experimental conditions: 2 μM TNP-ATP, 120 μg mL^{-1} protein, and 40 mM Tris-HCl at pH 7.4, and ambient temperature.

Phosphoenyme. The amount of acid-stable phosphoenzyme formed from 5 μM [γ-^{32}P]ATP was measured by quenching after 15 s with trichloroacetic acid containing cold ATP, collecting the precipitated membranes on a 3-μm Millipore filter, washing with trichloroacetic acid containing cold P_i, dispersing in scintillation fluid, and counting.

Results

Competitive Binding

TNP-ATP binding to the gastric H,K-ATPase has been characterized (Faller, 1989). Binding to apoenzyme (+EDTA) enhances the fluorescence of TNP-ATP 4.6-fold. The fluorescence enhancement (ΔF) reaches a maximum value (ΔF_{max}) at low concentrations of TNP-ATP (k_d < 25 nM), indicating binding to specific sites (N = 3.4 ± 0.9 nmol mg^{-1}).

Apoenzyme. Additional evidence for specific binding is shown in Figure 1. When apo-H,K-ATPase saturated with TNP-ATP is titrated with ATP, the fluorescence enhancement is completely reversed (open circles). The quench occurs over 2 log orders. The simplest explanation of this result is that ATP and the fluorescent substrate analogue compete for the same site or class of equivalent sites. This interpretation is strengthened in a subsequent section, where it is demonstrated that TNP-ATP competitively inhibits ATP hydrolysis. The result shown in Figure 1 demonstrates that TNP-ATP binding to apoenzyme is reversible, as well as specific.

The theoretical line through the open circles was calculated for ATP binding to a single class of sites with K_s(app) = 86 μM. Introducing the estimated maximum value of K_d for TNP-ATP binding into an expression with the same form as

[2] The subscript d is a general way of indicating that the equilibrium between enzyme and ligand (L) is written as a dissociation: EL ⇌ E + L. When L is a substrate or an inhibitor, it is conventional to substitute the subscript s or i and to refer to the equilibrium dissociation constant (K_d) as a substrate (K_s) or an inhibitor (K_i) constant (IUPAC/IUB Commission on Biochemical Nomenclature, 1973).

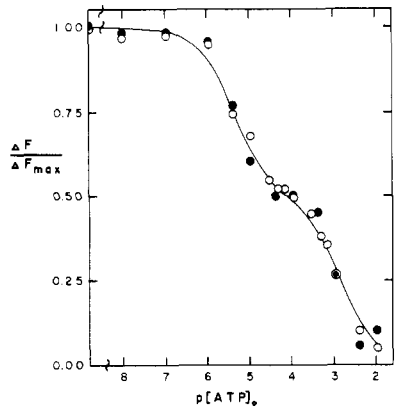

FIGURE 2: ATP displaces TNP-ATP biphasically when Mg^{2+} is present. TNP-ATP was added to enzyme in 2.8 mM $MgCl_2$. After the fluorescence intensity decayed to a stable level, the fluorophore–enzyme complex was titrated with ATP. The ordinate is fraction of enhancement in the Mg^{2+}-quenched state. The abscissa is $-\log [ATP]_0$. The open and solid circles are separate experiments. Equation 3 was used to calculate the theoretical curve for displacement from equivalent numbers of noninteracting sites with apparent substrate constants 4.5 μM and 1.5 mM. Other conditions: 2 μM TNP-ATP, 120 $\mu g\ mL^{-1}$ protein, 0.8 mM EDTA, and 40 mM Tris-HCl at pH 7.4 and ambient temperature.

eq 2 gives $K_s < 1$ μM for ATP dissociation from apoenzyme. ADP also displaces TNP-ATP. The maximum value of K_d estimated from the apparent dissociation constant was 6 μM, so ATP binds 6 times tighter than ADP. Vanadate inhibition of the H,K-ATPase can be explained by competitive binding with ATP (Faller et al., 1983). Therefore, the fluorophore–apoenzyme complex was also titrated with vanadate ions. Vanadate displaced TNP-ATP with $K_d < 94$ μM. The value of K_d for vanadate dissociation from apoenzyme estimated from direct binding measurements was 30 μM (Faller et al., 1983).

K^+ Enzyme. The solid circles in Figure 1 show that the fluorescence enhancement is also completely reversed when enzyme saturated with TNP-ATP in the presence of 7 mM K^+ is titrated with ATP. The total amplitude of the fluorescence change is about 30% less, because the enhancement factor (ratio of fluorescence intensities when the same amount of fluorophore is bound and free) is smaller in the K^+-quenched state (Faller, 1989). The titration is consistent with competition between ATP and TNP-ATP for a single class of nucleotide sites. The difference between the K_s(app) values (figure legend) that give the best fits to the displacement curves from apoenzyme and K^+ enzyme is marginally significant, indicating that any differences in affinity of the enzyme for ATP or TNP-ATP in the presence or absence of K^+ are slight. No effect of 7 mM K^+ on the affinity of the enzyme for TNP-ATP could be measured in direct titrations (Faller, 1989).

Mg^{2+} Enzyme. In sharp contrast to the behavior of K^+ enzyme and apoenzyme, Figure 2 shows that the concentration of ATP must be increased over 4 log orders to completely displace TNP-ATP from the gastric ATPase when Mg^{2+} is present. There is a slow fluorescence quench (about 40%) when Mg^{2+} and TNP-ATP are both bound (Faller, 1989). Therefore, enzyme was loaded by preincubating with Mg^{2+}, adding TNP-ATP, and waiting until the fluorescence intensity decayed to a stable level before beginning the titration with ATP. The solid and open circles are data from two separate titrations. In these experiments the concentration of free Mg^{2+} was effectively buffered until near the end of the second titration. In another experiment the Mg^{2+} concentration was increased to 5.8 mM to be sure Mg^{2+} chelation by ATP did not cause the second sigmoid. The shape of the titration curve did not change. In all, seven independent titrations were carried out with two different enzyme preparations.

The theoretical curve in Figure 2 was calculated from a least-squares fit of

$$\frac{\Delta F}{\Delta F_{max}} = 1 - \left[X_1 \frac{[ATP]_0}{[ATP]_0 + K_s(app)_1} + (1 - X_1) \frac{[ATP]_0}{[ATP]_0 + K_s(app)_2} \right] \quad (3)$$

to the data. That is, it was assumed that there are two noninteracting classes of ATP binding sites with apparent substrate constants $K_s(app)_1$ and $K_s(app)_2$ and that the fraction of the sites in the first class is X_1. Assuming half the sites are in each class gave $K_s(app)_1 = 7.1 \pm 4.5$ μM and $K_s(app)_2 = 1.4 \pm 0.7$ mM ($n = 7$) with a relative root mean square error of 3%. Since $N = 3.4$ nmol mg^{-1}, the concentration of sites was 0.4 μM, so at the midpoint of the first titration [ATP] equaled $[ATP]_0$ within 3%, and the error introduced by using the total titrant concentration in eq 3 is negligible. Letting X_1 vary did not improve the fits significantly and gave estimates of X_1 within 1 standard deviation of 0.5. Therefore, two equimolar classes of sites can adequately explain the experimental data.

There may be alternative explanations of the double titration in Figure 2, because the titrant is the substrate and Mg^{2+} activates the enzyme. For example, ADP produced during the experiment, or phosphorylation of the enzyme, might account for biphasic displacement of TNP-ATP. The simplest way to test these possibilities would be to displace TNP-ATP with ADP or another competitive inhibitor that cannot react with the enzyme. Therefore, the TNP-ATP-saturated, Mg^{2+}-quenched state was titrated with ADP and vanadate. The nucleotide only partially displaced TNP-ATP. ADP binds less tightly than ATP to apoenzyme, so the end point of the titration is probably outside the experimentally accessible ADP concentration range. Vanadate displaced TNP-ATP completely, but the titration curves could not be unambiguously interpreted. In the presence of Mg^{2+} alone, the midpoint of the titration was $p[H_2VO_4^-]_0 = 4.5$. K^+ shifted the midpoint to about $p[H_2VO_4^-]_0 = 5.8$, confirming that vanadate binds more tightly to the K^+ enzyme (Faller et al., 1983). The titration curves were broader than expected for binding to a single class of sites, but there was considerable scatter in the data, perhaps because vanadate equilibrates with the enzyme slowly, and it was not possible to resolve a definite inflection. Therefore, an explanation of the double displacement of TNP-ATP by ATP based on turnover of the substrate could not be excluded experimentally.

Inhibition of Catalysis

No catalysis of TNP-ATP hydrolysis was detected when 2 mM TNP-ATP was incubated with 10 $\mu g\ mL^{-1}$ H,K-ATPase at pH 7.4 in 2 mM Mg^+ and 7 mM K^+ for 0.5 h at 37 °C or for 1 h at 22 °C. Therefore, TNP-ATP is not a substrate for the gastric enzyme.

Phosphorylation. Figure 3 shows that TNP-ATP inhibits phosphorylation of the gastric ATPase. The maximum phosphoenzyme level in this experiment was 1.05 nmol mg^{-1}. The solid line was calculated for TNP-ATP binding with a single apparent inhibition constant K_i(app) = 0.36 μM. In the case of competitive inhibition, the expression relating the Michaelis constant for the phosphorylation reaction to the apparent and true inhibition constants has the same form as

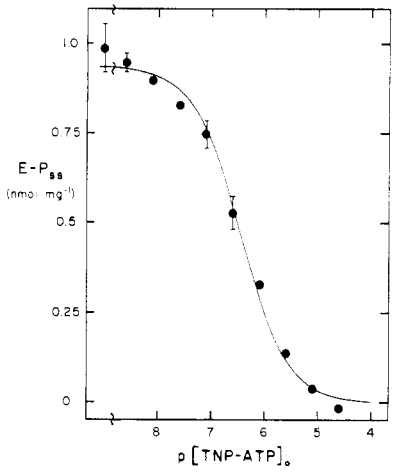

FIGURE 3: TNP-ATP inhibits phosphorylation of the H,K-ATPase. The steady-state level of phosphoenzyme ($E-P_{ss}$) is plotted against $p[TNP-ATP]_0 = -\log [TNP-ATP]_0$. Each point is the average of three measurements, and the vertical bars indicate the standard deviation in the amount of acid-precipitable phosphoenzyme formed. The theoretical curve was calculated for inhibition of phosphorylation by TNP-ATP binding to a single class of sites with K_I(app) = 0.36 μM. Other conditions: 5 μM [γ-^{32}P]ATP, 2 mM $MgCl_2$, 47 μg mL^{-1} protein, and 40 mM Tris-HCl at pH 7.4 and ambient temperature.

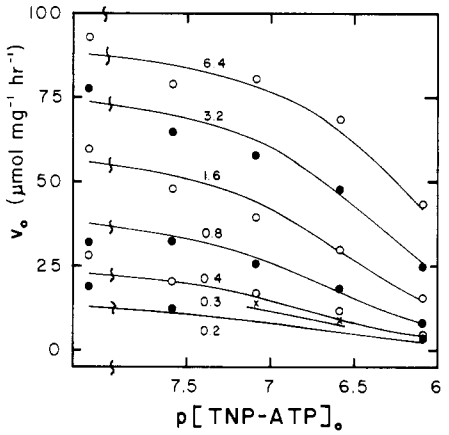

FIGURE 4: TNP-ATP competitively inhibits the pNPPase activity of the gastric H,K-ATPase. Initial velocity (v_0) is plotted against $p[TNP-ATP]_0 = -\log [TNP-ATP]_0$. $[pNPP]_0$ (mM) is given on the graph. Equation 1 was used to calculate theoretical curves for competitive inhibition. The kinetic parameters that gave the best fit are recorded in Table I. Other conditions: 5 μg mL^{-1} protein, 7 mM KCl, 2 mM $MgCl_2$, and 40 mM Tris-HCl at pH 7.4 and 37 °C.

eq 2 with the roles of substrate and inhibitor interchanged (Segel, 1975). The maximum value of K_m (0.37 μM) calculated for K_i < 25 nM falls between the smaller Michaelis constant (K_{m1} = 0.4 μM) estimated from the kinetics of the hydrolysis reaction (Wallmark et al., 1980) and the smaller substrate constant (K_{s1} < 0.09 μM) deduced from the titration in Figure 2 by assuming competitive binding (see Discussion).

pNPPase Activity. The H,K-ATPase also catalyzes hydrolysis of pNPP. A phosphoenzyme intermediate has not been demonstrated, but ATP inhibits competitively (Forte et al., 1981). There is agreement that the substrate dependence of the reaction can be described by a single Michaelis constant in the range 0.9 mM (Schrijen, 1981) to 1.44 mM (Forte et al., 1981). Figure 4 shows that TNP-ATP inhibits the K^+-stimulated pNPPase activity of the gastric enzyme. The reaction was studied as a function of substrate and inhibitor concentrations over the ranges $0.2 \leq [pNPP]_0 \leq 6.4$ mM and $0 \leq [TNP-ATP]_0 \leq 1$ μM. Each experimental point in the figure is the mean of three measurements. The theoretical curves were calculated with eq 1 and demonstrate that competitive inhibition adequately describes the results. The root mean square error expressed as a percentage of the maximum velocity is only 3.0%. The estimated parameters are reported in Table I. The estimated Michaelis constant (K_m = 1.48 ± 0.15 mM) falls within the published range.

Table I: Summary of Kinetic Parameters[a]

substrate	V (μmol mg^{-1} h^{-1})	K_m (mM)	K_i (μM)	RRMSE[b] (%)
pNPP	108 ± 4	1.48 ± 0.15	0.14 ± 0.02	3.0
low ATP	117 ± 6	0.10 ± 0.01	0.42 ± 0.04	2.3
high ATP	184 ± 11	0.26 ± 0.05	0.38 ± 0.07	5.0

[a] Value ± standard error predicted by eq 1 for competitive inhibition. Experimental conditions: 5 μg mL^{-1} protein, 7 mM KCl, 2 mM $MgCl_2$, 40 mM Tris-HCl at pH 7.4 and 37 °C. Substrate and inhibitor concentration ranges are given in the text and in Figures 4–6. [b] Relative root mean square error [=100(RMSE/V)].

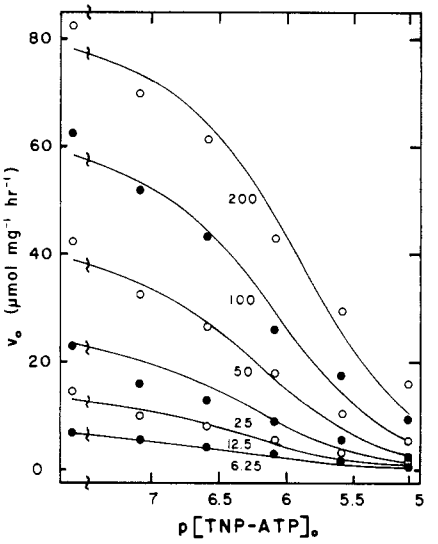

FIGURE 5: TNP-ATP competitively inhibits the H,K-ATPase at low ATP concentrations. $[ATP]_0$ (μM) is given on the graph. The meaning of the coordinate axes is explained and other experimental conditions are given in the legend to Figure 4. The kinetic parameters estimated by fitting the data to eq 1 are reported in Table I.

ATPase Activity. ATP hydrolysis was investigated at both high and low substrate concentrations to see if the inhibition pattern corroborates the evidence in Figure 2 that TNP-ATP and ATP compete at sites with different affinities for the substrate. Optimum reaction conditions (pH 7.4 and 37 °C in 2 mM Mg^{2+} and 7 mM K^+) were chosen in order to have accurately measureable rates. Under these conditions two Michaelis constants fit the data better than one. The values range from 17 to 74 μM for the higher affinity site and from 0.47 to 1.1 mM for the lower affinity site (Sachs et al., 1980; Schrijen, 1981). The substrate concentration ranges bracketing these values were studied separately using a radioassay in the lower concentration range to increase sensitivity. Overlapping concentration points were used to normalize the two sets of rate data.

Figure 5 shows the results obtained in the low concentration range, $6.25 \leq [ATP]_0 \leq 200$ μM. Measurements were made in triplicate. Equation 1 was used to calculate theoretical titration curves. The parameters that gave the best fit are recorded in Table I. The root mean square error is 2.7. This measure of agreement between experiment and theory increases if noncompetitive inhibition is assumed.

Figure 6 shows the data in the high concentration range, $0.2 \leq [ATP]_0 \leq 3.2$ mM. Except for the two points at 3.2 mM ATP_0, Mg^{2+} was always in excess. Triplicate measurements were averaged. The parameters estimated by a non-

Table II: Stoichiometry of Inhibitor Binding to the Gastric H,K-ATPase

inhibitor	N (nmol mg^{-1})	E–P[a] (nmol mg^{-1})	N/E–P	reference
AMP-PNP	2–3.5	0.7–1.5	2.5	Schrijen (1981); Van De Ven et al. (1981)
TNP-ATP	3.4 ± 0.9 (n = 21)	1.5	2.3	Faller (1981)
$H_2VO_4^-$	2.8 ± 0.3	1.5 ± 0.3 (n = 41)	1.9	Faller et al. (1983)
eosin Y	3.5	1.4	2.5	Helmich-de Jong et al. (1986)
FITC	1.5 ± 0.2 (n = 4)	0.64	2.3	Jackson et al. (1983)
FITC	3.5 ± 1.6 (n = 3)	1.5	2.3	Farley and Faller (1985)
omeprazole	2	1	2	Lorentzon et al. (1987)

[a] Formed from ATP.

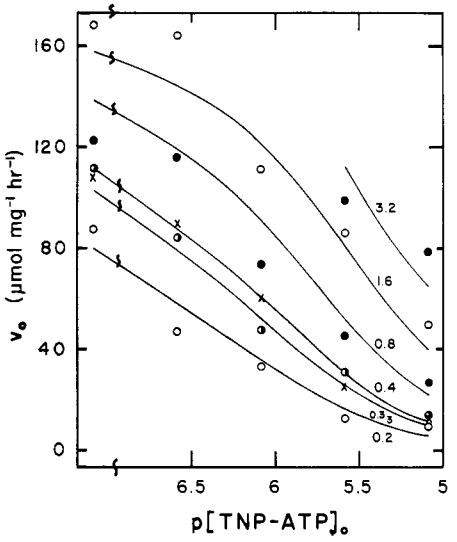

FIGURE 6: TNP-ATP competitively inhibits the H,K-ATPase at high ATP concentrations. $[ATP]_0$ (mM) is given on the graph. Other details of the plot are given in the legend to Figure 4, and the kinetic parameters used to draw the theoretical curves are reported in Table I.

linear least-squares fit of eq 1 to the data are given in Table I, and theoretical curves are shown in the figure. The maximum velocity (V) equals 184 μmol mg^{-1} h^{-1}. The relative root mean square error is 5.0%.

Equation 1 satisfactorily describes the ATPase activity of the gastric enzyme in both the high and low substrate concentration ranges. The K_i estimated by both data sets is the same, consistent with evidence from binding experiments for only one class of inhibitor sites (Faller, 1989). However, statistically different Michaelis constants are estimated. K_{m1} = 100 μM is larger than published values (17 ≤ K_{m1} ≤ 74 μM), and K_{m2} = 0.26 mM is smaller than published values (0.47 ≤ K_{m2} ≤ 1.1 mM). Two affinities for ATP could explain two Michaelis constants. One way to account for two affinities is to postulate two classes of nucleotide sites. Therefore, both the kinetic inhibition data and the binding data in Figure 2 are consistent with competition between ATP and TNP-ATP for two classes of nucleotide sites. Alternative interpretations are considered under Discussion.

Discussion

In a related paper the fluorescent substrate analogue TNP-ATP was used to count the number of nucleotide sites on the H,K-ATPase and shown to report cofactor-induced changes in the enzyme's conformation (Faller, 1989). The competition experiments described in this paper confirm that TNP-ATP binds specifically and provide additional reasons for interpreting the stoichiometry of TNP-ATP binding as evidence for two classes of nucleotide sites.

Characteristics of TNP-ATP Binding. Stoichiometric amounts of TNP-ATP saturate the enzyme, so it was concluded that binding is specific. Two additional arguments that TNP-ATP binds to specific nucleotide sites are presented under Results of this paper. First, ATP displaces TNP-ATP (Figure 1). Second, TNP-ATP competitively inhibits the enzyme (Figures 4–6). These two observations also demonstrate that TNP-ATP binding is reversible. The simplest interpretation of the data is that ATP and TNP-ATP compete for the same sites, although mutually exclusive binding to different sites is an alternative possibility.

TNP-ATP binding could be described by an equation derived for binding to a single class of sites, so it was concluded that TNP-ATP binds with a single affinity. The competition experiments reported here strengthen that interpretation. First, TNP-ATP inhibits ATP hydrolysis with a single K_i (Table I). Second, ATP binds to apoenzyme and displaces TNP-ATP with a single apparent substrate constant (Figure 1). ATP also displaces TNP-ATP from the quenched K^+ state monophasically (solid circles). The double-displacement curve in Figure 2 for TNP-ATP loss from the quenched Mg^{2+} state could be attributed to two TNP-ATP affinities. However, in the next section it will be argued that two ATP affinities are a better explanation, because there is independent evidence for two substrate affinities of the right magnitude when Mg^{2+} is present.

Evidence for Two Classes of Substrate Sites. The first result suggesting two classes of substrate sites is that the stoichiometry of TNP-ATP binding to the H,K-ATPase is twice the stoichiometry of phosphoenzyme formation. The stoichiometry estimated for TNP-ATP binding to enzyme that forms a maximum of 1.5 ± 0.3 nmol mg^{-1} of phosphoenzyme (Faller et al., 1983) was 3.4 ± 0.9 nmol mg^{-1} (Faller, 1989).

Other stoichiometries for inhibitors of the gastric enzyme that have been reported in the refereed literature are collected in Table II for comparison. Reagents that inhibit by a variety of mechanisms are included. The first two inhibitors in the table are substrate analogues. $H_2VO_4^-$ stereochemically resembles inorganic phosphate, one of the products of ATP hydrolysis. Eosin reportedly competes with ATP, even though it does not resemble either substrate or product structurally. The last two inhibitors in the table chemically modify the enzyme. FITC, which is structurally related to eosin, is thought to react at or near the active site, because substrate protects against covalent incorporation of fluorescein. Omeprazole inhibits by reacting with a cysteine residue on the opposite side of the membrane from the active site. The maximum phosphorylation levels of the enzyme preparations are also tabulated. In the absence of K^+, dephosphorylation is rate-limiting, so the amount of phosphoenzyme formed from [γ-^{32}P]ATP equals the stoichiometry of phosphorylatable sites (Wallmark & Mardh, 1979).

Despite the diversity of reagents, there is remarkable agreement on the stoichiometry of inhibition. There is even greater agreement on the ratio of inhibitor stoichiometry to phosphoenzyme stoichiometry. This ratio is more meaningful than either stoichiometry alone, because the numerical values of N and E–P depend on the purity of the enzyme preparation

Table III: Comparison of Published Michaelis Constants with Binding and Kinetic Parameters Estimated by Assuming Competition between TNP-ATP and ATP[a]

		predicted		reported K_m		
experiment	figure	K_s (μM)	K_m (mM)	μM	mM	reference
ATP binding[b]	2	<0.09		0.4		Wallmark et al. (1980)
		<18		50		
phosphorylation[b]	3	<0.37		0.4		Wallmark et al. (1980)
pNPP hydrolysis[c]	4		1.48		0.9	Schrijen (1981)
					1.44	Forte et al. (1981)
ATP hydrolysis[c]	5		0.10		0.017	Schrijen (1981)
					0.074	Sachs et al. (1980)
	6		0.26		0.47	Schrijen (1981)
					1.1	Sachs et al. (1980)

[a] Comparable experimental conditions. Exact details given in figure legend or reference. [b] Cofactor Mg^{2+} at ambient temperature. [c] Cofactors K^+ and Mg^{2+} at 37 °C.

and the method used to assess protein content. These uncertainties cancel out when nucleotide and phosphorylation stoichiometries measured in the same laboratory on the same enzyme preparations are compared. The fact that the N/E–P ratio is also 2, within experimental error, for the other inhibitors in Table II strengthens the interpretation of the TNP-ATP binding stoichiometry as evidence for two nucleotide sites per phosphorylation site.

The second indication there are two classes of substrate sites is the double titration in Figure 2. The theoretical curve in the figure was drawn by assuming two equimolar classes of noninteracting ATP sites (eq 3). It is possible to assess whether the estimated, apparent substrate constants are sensible. Assuming competitive binding and negligible turnover, they are related to substrate constants by equations having the same form as eq 2 with $K_d < 25$ nM, since there is evidence for only one class of TNP-ATP sites. In Table III the upper estimates for K_{s1} and K_{s2} are compared with Michaelis constants deduced from the substrate dependence of the Mg^{2+}-ATPase reaction. The agreement is remarkably good. That is, kinetic evidence for two substrate affinities already in the literature not only predicts the qualitative shape of the titration curve in Figure 2 but also gives consistent quantitative estimates for the midpoints of the two titrations.

It is quite possible that TNP-ATP binds equivalently and ATP binds nonequivalently to the same sites, because their structures are different. The substrate analogue binds over an order of magnitude more tightly than ATP, so the trinitrophenyl group must be important in determining the stability of the analogue–enzyme complex. Therefore, the data in Figure 2 can be plausibly explained by two noninteracting classes of nucleotide sites with different affinities for ATP, but the same affinity for TNP-ATP. Anticooperative binding of ATP in the presence of Mg^{2+} is also a possibility.

Alternative explanations of the result in Figure 2 based on ATP turnover could not be excluded experimentally by demonstrating biphasic displacement of TNP-ATP with ADP or $H_2VO_4^-$. The quench of TNP-ATP fluorescence by low concentrations of nucleotides described in a preliminary paper (Sartor et al., 1982), and illustrated for vanadate in Figure 9 of a review written by the author (Faller et al., 1985), probably resulted from the slow Mg^{2+} quench pictured in the related paper on TNP-ATP binding (Faller, 1989). The biphasic quench shown in Figure 2 of this paper cannot be explained by a slow time-dependent change superimposed on competitive binding to a single class of sites, because after TNP-ATP and Mg^+ were added, the fluorescence intensity was allowed to decay to a stable level before the reported titrations with ATP were begun.

Explanations of the result in Figure 2 based on enzymatic turnover are unlikely on theoretical grounds. ATP hydrolysis could account for the biphasic titration in either of two ways. First, half the TNP-ATP might be displaced by ATP and the other half by ADP formed during the titration. No quench was observed below $p[ATP]_0 = 5$ when the Mg^{2+} enzyme was titrated with ADP, so ADP did not cause the first sigmoid. At the midpoint of the second titration less than 20% of the ATP was hydrolyzed. This is a generous estimate made by ignoring TNP-ATP inhibition of hydrolysis and assuming a basal Mg^{2+}-ATPase activity of 3 μmol mg^{-1} h^{-1}. Therefore, in addition to binding less tightly than ATP, ADP was present at lower concentration, so it is unlikely ADP binding caused the second sigmoid. Second, phosphorylation of the enzyme by ATP could explain Figure 2, if TNP-ATP remained bound and was displaced by ATP with different apparent affinity. This possibility is unlikely, because TNP-ATP prevents phosphorylation (Figure 3). If phosphorylation did occur, all the reactive sites should be phosphorylated, because phosphorylation is reportedly 1–2 orders of magnitude faster than dephosphorylation in the absence of K^+ (Wallmark & Mardh, 1979; Wallmark et al., 1980). Therefore, even if phosphorylation were responsible for the double titration in Figure 2, two classes of nucleotide sites would be needed to explain TNP-ATP and ATP binding to phosphoenzyme or phosphorylation of only half the sites.

The final evidence for two nucleotide sites is that inhibition data in the high and low substrate concentration ranges give different estimates for the Michaelis constant (Table I). The ratio K_{m2}/K_{m1} is not as large as previously reported (Table III). That may simply be because the published values were inferred from curved v_0 vs $v_0/[S]_0$ plots. This curvature is greater when K^+ is omitted (Wallmark et al., 1980), but then it is hard to exclude the possibility that a Mg^{2+}-ATPase impurity in the preparation caused the curvature. TNP-ATP inhibition of K^+-activated ATPase activity was studied to avoid this uncertainty. The predicted Michaelis constants are sufficiently resolved to strengthen the conclusion that there are two substrate affinities. A single K_i gave the best fits to both sets of ATPase data. The predicted value of K_i at 37 °C is bigger than the maximum value of K_d measured at ambient temperature. An increase in K_d with increasing temperature is qualitatively what is expected for a bimolecular reaction between a macromolecule and a small molecule.

One possible inconsistency in the data is the smaller K_i estimated for inhibition of pNPPase activity. If ATP and pNPP react with the same form of the enzyme, K_i should be the same for both activities. Fixing $K_i = 0.4$ μM increased the predicted K_m to 2.3 mM and the relative root mean square error to 5.0%, which is still an acceptable uncertainty for enzyme kinetic measurements. Alternatively, pNPP and ATP might react with different forms of the enzyme. For example, pNPP is sometimes shown reacting with the E_2 conformer (de

Jong, 1986), presumably without going through E_1 or forming a covalent phosphoenzyme intermediate.

Conclusions about H,K-ATPase. There have been repeated suggestions that the functional H,K-ATPase is a dimer (Faller et al., 1985). This idea is supported by two kinds of evidence: first, evidence for two nucleotide sites, and second, evidence the functional molecular weight is a multiple of 114000. TNP-ATP interaction with the H,K-ATPase adds to the evidence in support of the major arguments favoring two substrate sites.

Stoichiometries must be interpreted with caution, especially when the measured stoichiometry (3.4 nmol/mg of Lowry protein) is less than half the theoretical stoichiometry (8.8 nmol/mg of 114000 polypeptide). However, many of the factors that could account for this difference cancel out of the ratio N/E–P, which equals 2.3 ± 0.2 (n = 7) for a diverse group of inhibitors of the gastric ATPase including TNP-ATP (Table II). The implication of this ratio is that the reactivity of half the sites is different.

Two nucleotide sites were originally proposed to explain curved v_0 vs $v_0/[S]_0$ plots (Wallmark et al., 1980; Schrijen, 1981). There is also a consensus now that better analytical fits are obtained with a rate expression containing $[S]_0^2$ terms than with the Michaelis–Menten equation (Ljungstrom & Mardh, 1985; Reenstra et al., 1988). The TNP-ATP inhibition data in Figures 5 and 6 support the conclusion there are two sites, but illustrates the inherent weakness of kinetic evidence in the case of the gastric ATPase. Two Michaelis constants are estimated (Table I), but their ratio (2.6) approaches the lower limit that can be statistically resolved.

More compelling evidence for two nucleotide sites comes from competition experiments in which two apparent constants for binding to the gastric ATPase, or inhibition of catalytic activity, differ by more than 2 orders of magnitude. ATP displaces TNP-ATP biphasically from the Mg^{2+}-quenched form of the enzyme (Figure 2). The ratio of the apparent substrate constants used to draw the theoretical curve in the figure is over 300. Also cleanly resolved, in both the presence and absence of K^+, are two apparent constants for vanadate inhibition of the gastric ATPase and vanadate binding to the enzyme (Faller et al., 1983).

The two substrate constants deduced from the double-titration curve in Figure 2 are in satisfactory agreement with published Michaelis constants (Table III). Two Michaelis constants can result from two states of a single site in different conformers of an enzyme with different affinities for substrate (Smith et al., 1980). However, the one-site, two-state model cannot explain the biphasic quench of TNP-ATP fluorescence shown in Figure 2 for the same reason it could not explain vanadate inhibition of the gastric ATPase (Faller et al., 1983). ATP binding to the conformer with higher relative affinity for substrate would shift the equilibrium between the enzyme forms, so that all the TNP-ATP was displaced with a single apparent affinity for ATP. It has been proposed that H^+ and K^+ regulate the gastric ATPase (Ljungstrom et al., 1984; Ljungstrom & Mardh, 1985). In this model hydrogen and potassium forms of the enzyme have different affinities for ATP. That idea cannot explain either the ATP quench of TNP-ATP fluorescence in Figure 2 or vanadate inhibition of the enzyme, because both are biphasic in the absence of K^+.

More generally, it has been argued that the one-site, two-state model is simpler than a two-site mechanism (Norby, 1983). That is not true mathematically, because in the one-site, two-state model there is an additional parameter that specifies the distribution of the enzyme between the two forms. This point is illustrated by the ATP quench of TNP-ATP fluorescence. When X_1 in eq 3 was permitted to vary from 0.5, the fit was not significantly improved. Two affinities for ATP are adequate to explain the data in Figure 2. The two-site model is simpler, because the number of sites of each type is constrained to be the same. This condition is met for vanadate binding and inhibition of the H,K-ATPase (Faller et al., 1983), as well as competitive binding of ATP and TNP-ATP to the Mg^{2+}-quenched state (Figure 2).

It might be simpler if both nucleotide sites were located on the same polypeptide chain. However, radiation inactivation of the gastric enzyme invariably occurs with cross sections corresponding to multimeric structures. The target size of lyophilized preparations indicated the enzyme is a trimer (Saccomani et al., 1981) or a tetramer (Peters et al., 1982). More recently, frozen preparations have been studied. The measured target size for loss of ATPase activity was 232000 ± 23000, exactly twice the molecular weight inferred from the primary structure of the enzyme (Shull & Lingrel, 1986) and significantly larger than the target size for inhibition of phosphoenzyme formation, suggesting the structure that turns over is a dimer (Kempner and Rabon, priate communication). Therefore, the most self-consistent interpretation of the evidence for two nucleotide sites and a multimeric structure is that the sites are on different polypeptide chains.

Comparison with Other E_1E_2-ATPases. The conclusion drawn from studies of TNP-ATP binding to the Na,K-ATPase was that there is a single nucleotide site on the catalytic subunit with different affinities for ATP in the E_1 and E_2 conformers, depending on the metal cofactors present (Moczydlowski & Fortes, 1981a,b). Since a different conclusion has been reached in the case of the H,K-ATPase, it is important to stress that fundamentally different experimental results were obtained with the two enzymes. First, in contrast to the N/E–P ratio of 2 found for TNP-ATP and a variety of other inhibitors of the H,K-ATPase, the stoichiometry of TNP-ATP binding to the Na,K enzyme approximately equaled the stoichiometry of ouabain binding, which in turn equals the stoichiometry of phosphoenzyme formation (Peters et al., 1981). Second, in contrast to the displacement curves shown in Figure 2 for the gastric ATPase, ATP and TNP-ATP competed for a single site on the Na,K-ATPase regardless of the cofactor present. Finally, in contrast to the kinetic result shown in Figure 5, noncompetitive or mixed inhibition of the Na,K-ATPase was observed at low ATP concentrations. The underlying mechanism of cofactor-induced changes in TNP-ATP fluorescence has been shown to be different in the cases of the H,K-ATPase and Na,K enzyme (Faller, 1989).

On the other hand, the results obtained in this study of the H,K-ATPase are similar to reports of TNP-nucleotide binding to the SR Ca-ATPase. First, the stoichiometry of TNP-nucleotide binding to the Ca-ATPase is approximately twice the phosphorylation capacity of the enzyme in most accounts (Dupont et al., 1982, 1985; Wanatabe & Inesi, 1982; Nakamoto & Inesi, 1984; Bishop et al., 1984), although one report claims they are the same (Bishop et al., 1987). Second, ATP displaces TNP-nucleotides from the Ca-ATPase biphasically (Wanatabe & Inesi, 1982; Dupont et al., 1985). Figure 2b in the latter reference is quite similar to Figure 2 of this paper. In the presence of Mg^{2+} β,γ-imino-ATP is chased from Ca-ATPase by ATP with two apparent substrate constants differing by more than 2 orders of magnitude. The consensus is that the Ca-ATPase has catalytic and regulatory nucleotide sites. Whether they are distinct sites or different states of the same site is unresolved. Phosphorylation of the Ca-ATPase

causes a large, additional enhancement of bound TNP-nucleotide fluorescence (Dupont & Pougeois, 1983; Nakamoto & Inesi, 1984; Bishop et al., 1984; Berman, 1986) that is not seen with either the Na,K-ATPase (Moczydlowski & Fortes, 1981a), or the H,K-ATPase (Figure 2). A recent paper explains this increase in fluorescence by TNP-nucleotide binding to phosphoenzyme at the active site in place of ADP and equates the regulatory site with the phosphorylated catalytic site (Bishop et al., 1987).

ACKNOWLEDGMENTS

I am indebted to Terry J. Reedy for help with the statistical analysis, to Drs. Sartor, Saccomani, and Sachs for access to their unpublished work, and to George Sachs, who organized the program project that provided partial support for the initial phase of this investigation.

Registry No. Na,K-ATPase, 9000-83-3; 5′-ATP, 56-65-5; TNP-ATP, 120360-48-7; pNPPase, 9073-68-1; pNPP, 330-13-2.

REFERENCES

Berman, M. C. (1986) *J. Biol. Chem. 261*, 16494–16501.
Bishop, J. E., Johnson, J. D., & Berman, M. C. (1984) *J. Biol. Chem. 259*, 15163–15171.
Bishop, J. E., Al-Shawi, M. K., & Inesi, G. (1987) *J. Biol. Chem. 262*, 4658–4663.
de Jong, M. (1986) Ph.D. Dissertation, University of Nijmegen, The Netherlands.
Dupont, Y., & Pougeois, R. (1983) *FEBS Lett. 156*, 93–98.
Dupont, Y., Chapron, Y., & Pougeois, R. (1982) *Biochem. Biophys. Res. Commun. 106*, 1272–1279.
Dupont, Y., Pougeois, R., Ronjat, M., & Verjovsky-Almeida, S. (1985) *J. Biol. Chem. 269*, 7241–7249.
IUPAC/IUB Commission on Biochemical Nomenclature (1973) *Enzyme Nomenclature*, pp 28–31, Elsevier Scientific Publishing, New York.
Faller, L. D. (1989) *Biochemistry* (submitted for publication).
Faller, L. D., Rabon, E., & Sachs, G. (1983) *Biochemistry 22*, 4676–4685.
Faller, L. D., Smolka, A., & Sachs, G. (1985) *The Enzymes of Biological Membranes* (Martonosi, A. N., Ed.) Vol. 3, pp 431–448, Plenum Publishing, New York.
Farley, R. A., & Faller, L. D. (1985) *J. Biol. Chem. 260*, 3899–3901.
Forte, J. G., Poulter, J. L., Dykstra, R., Ribas, J., & Lee, H. C. (1981) *Biochim. Biophys. Acta 644*, 257–265.
Helmich-de Jong, M. L., van Duynhoven, J. P. M., Schuurmans Stekhoven, F. M. A. H., & De Pont, J. J. H. H. M. (1986) *Biochim. Biophys. Acta 858*, 254–262.
Inesi, G., Goodman, J. J., & Watanabe, S. (1967) *J. Biol. Chem. 242*, 4637–44643.
Jackson, R. J., Mendlein, J., & Sachs, G. (1983) *Biochim. Biophys. Acta 731*, 9–15.
Kanazawa, T., Saito, M., & Tonomura, Y. (1970) *J. Biochem. 67*, 693–711.
Ljungstrom, M., & Mardh, S. (1985) *J. Biol. Chem. 260*, 5440–5444.
Ljungstrom, M., Vega, F. V., & Mardh, S. (1984) *Biochim. Biophys. Acta 769*, 220–230.
Lorentzon, P., Jackson, R., Wallmark, B., & Sachs, G. (1987) *Biochim. Biophys. Acta 897*, 41–51.
Lowry, O. H., Rosenbrough, N. J., Farr, A. L., & Randall, R. J. (1951) *J. Biol. Chem. 193*, 265–275.
Moczydlowski, E. G., & Fortes, P. A. G. (1981a) *J. Biol. Chem. 256*, 2346–2356.
Moczydlowski, E. G., & Fortes, P. A. G. (1981b) *J. Biol. Chem. 256*, 2357–2366.
Nakamoto, R. K., & Inesi, G. (1984) *J. Biol. Chem. 259*, 2961–2970.
Norby, J. G. (1983) *Curr. Top. Membr. Transp. 19*, 281–314.
Peters, W. H. M., Swarts, H. G. P., de Pont, J. J. H. H. M., Schuurmans Stekhoven, F. M. A. H., & Bonting, S. L. (1981) *Nature 290*, 338–339.
Peters, W. H. M., Fleuren-Jakobs, A. M. M., Schrijen, J. J., De Pont, J. J. H. H. M., & Bonting, S. L. (1982) *Biochim. Biophys. Acta 690*, 251–260.
Reenstra, W. W., Bettencourt, J. D., & Forte, J. G. (1988) *Biophys. J. 53*, 138a.
Saccomani, G., Sachs, G., Cuppoletti, J., & Jung, C. Y. (1981) *J. Biol. Chem. 256*, 7727–7729.
Sachs, G., Berglindh, T., Rabon, E., Stewart, H. B., Barcellona, M. L., Wallmark, B., & Saccomani, G. (1980) *Ann. N.Y. Acad. Sci. 341*, 312–334.
Sartor, G., Mukidjam, E., Faller, L., Saccomani, G., & Sachs, G. (1982) *Biophys. J. 37*, 375a.
Schrijen, J. I. (1981) Ph.D. Dissertation, University of Nijmegen, The Netherlands.
Segel, I. H. (1975) *Enzyme Kinetics*, pp 100–111, Wiley, New York.
Shull, G. E., & Lingrel, J. B. (1986) *J. Biol. Chem. 261*, 16788–16791.
Smith, R. L., Zinn, K., & Cantley, L. C. (1980) *J. Biol. Chem. 255*, 9852–9859.
Van De Ven, F. J. M., Schrijen, J. J., De Pont, J. J. H. H. M., & Bonting, S. L. (1981) *Biochim. Biophys. Acta 640*, 487–499.
Wallmark, B., & Mardh, S. (1979) *J. Biol. Chem. 254*, 1189–11902.
Wallmark, B., Stewart, H. B., Rabon, E., Saccomani, G., & Sachs, G. (1980) *J. Biol. Chem. 255*, 5313–5319.
Watanabe, T., & Inesi, G. (1982) *J. Biol. Chem. 257*, 11510–11516.
Yamamato, T., & Tonomura, Y. (1967) *J. Biochem. 62*, 558–575.
Yoda, A., & Hokin, L. E. (1980) *Biochem. Biophys. Res. Commun. 40*, 880–884.